J Appl Electrochem (2011) 41:633–643
DOI 10.1007/s10800-011-0276-1

ORIGINAL PAPER

# Sulfuric acid–methanol electrolytes as an alternative to sulfuric–hydrofluoric acid mixtures for electropolishing of niobium

**Xin Zhao · Sean G. Corcoran · Michael J. Kelley**

Received: 27 October 2010 / Accepted: 20 February 2011 / Published online: 18 March 2011


**Abstract** Attainment of the greatest possible interior surface smoothness is critical to meeting the performance demands placed upon niobium superconducting radiofrequency (SRF) accelerator cavities by next generation projects. Electropolishing with HF–$H_2SO_4$ electrolytes yields cavities that meet SRF performance goals, but a less-hazardous, more environmentally-friendly process is desirable. Reported studies of EP on chemically-similar tantalum describe the use of sulfuric acid–methanol electrolytes as an HF-free alternative. Reported here are the results of experiments on niobium samples with this electrolyte. Voltammetry experiments indicate a current plateau whose voltage range expands with increasing acid concentration and decreasing temperature. Impedance spectroscopy indicates that a compact salt film is responsible for the current plateau. Equivalent findings in electropolishing chemically-similar tantalum with this electrolyte were interpreted due to as mass transfer limitation by diffusion of Ta ions away from the anode surface. We infer that a similar mechanism is at work here. Conditions were found that yield leveling and brightening comparable to that obtained with HF–$H_2SO_4$ mixtures.

X. Zhao · S. G. Corcoran · M. J. Kelley
Department of Materials Science and Engineering,
Virginia Tech, Blacksburg, VA 24060, USA

M. J. Kelley (✉)
Applied Science Department, College of William and Mary,
Williamsburg, VA 23187, USA
e-mail: mkelley@jlab.org

M. J. Kelley
Thomas Jefferson National Accelerator Facility, Newport News,
VA 23606, USA

**Keywords** Electropolish · Niobium · SRF accelerator cavity

## 1 Introduction

The world-wide science community looks forward to a slate of accelerator-based user-facility projects of unprecedented magnitude and diversity, ranging from high energy physics to fourth generation light sources. Their success requires historically high performance and low unit cost. Most of these machines will be based on super-conducting radio frequency (SRF) niobium cavity accelerators. Recent reviews indicate that important problems are performance decline with increasing accelerator gradient and residual surface resistance beyond that predicted by the BCS model of superconductivity [1, 2]. A widely recognized contributor is cavity interior surface roughness, even down to nanoscale [3–5].

Accordingly, SRF researchers devote much attention to the final cavity interior surface conditioning step, removal of an approximately 100 μm-thick damage layer by chemical etching. The standard technique for cavity production up to now has been buffered chemical polishing (BCP). It circulates through the cavity interior a solution of 1:1:1 or 1:1:2 (volume ratio) $HNO_3$ (69%), HF (49%), and $H_3PO_4$ (85%) at approximately 10 °C. 1:1:2 BCP typically results in a Nb dissolution rate of about 1.5 μm $min^{-1}$ and a micron-scale surface roughness [6].

Seeking greater smoothness, electropolishing (EP) is now being introduced for routine production. The present EP process was initiated at Siemens in the 1970s [7] and was further developed by KEK in collaboration with Namura Plating Company [8]. Typically, a mixture of hydrofluoric (49%) and sulfuric acid (95–98%) at a volume

ratio of 1:9 is used with a temperature range of 30–40 °C, a current density of 30–100 mA $cm^{-2}$, and a total cell voltage of 10–20 V. The surface area ratio of the Nb cavity (anode) to the high purity Al tube cathode is 10:1 during practical cavity EP processing. The most common set-up places the cavity axis horizontal with the cathode tube on the axis. Fluid enters through cathode via a port at each cell and exits through the beam tubes at each end. The cavity is only about 60% filled to facilitate the exit of hydrogen produced at the cathode and rotates at about 1 RPM. Researchers at Cornell University Laboratory for Elementary Particle Physics (LEPP), have described an alternative EP process configuration, wherein the cavity is fixed with its axis vertical [9, 10]. In addition to being mechanically simpler, vertical EP permits steady-state, rather than interrupted, polishing conditions to be established at the cavity surface and can more readily accommodate external cooling for better process temperature control. The present state is that SRF cavities produced at Thomas Jefferson National Laboratory (JLab) and Deutsches Electronen-Synchrotron Laboratory (DESY) pilot EP facilities are meeting performance goals. A scale-up facility to enable routine cavity production by the vertical EP process is under construction at JLab, aiming to begin initial operation in 2011. Our present study is therefore directed toward a process that could be implemented there.

We recently reported work aimed at attaining detailed understanding of the HF–$H_2SO_4$ EP process based on multi-electrode cell studies and electrochemical impedance spectroscopy (EIS) [11]. Briefly, studies using three (or more) electrodes place an added (reference) electrode adjacent to the anode or (and) cathode, so that the potential drop at each and across the solution can be measured independently, in contrast with simply measuring their sum as a cell voltage and current, as has been done in previous Nb EP studies. Important findings include: (1) the cathode potential drop is purely resistive (current varies linearly with voltage) and not a major contributor to the cell voltage, even though its area is small ($\sim$10%) relative to the Nb anode; (2) the voltage drop across the solution is a few volts and is purely resistive (3) the anode shows a plateau (current constant with increasing voltage) from 2–3 V out to near 15 V. The plateau current increases with stirring, increases linearly with HF content, and increases exponentially with temperature, pointing to fluoride diffusion as rate limiting (mass transfer control). The EIS findings can be accounted for only by formation in the plateau region of a compact salt film on the anode surface. These results are consistent with the accepted understanding of topography control during anodic EP [12, 13].

Matlosz [13] has described the present mechanistic understanding of EP as mass transfer limitation of anodic dissolution along the limiting current plateau. Effects are evident at two dimensional scales. (1) Macrosmoothing is interpreted as the preferential dissolution of protrusions on the order of the diffusion layer due to their greater accessibility for diffusive transport. The mass transport limitation could be out-diffusion of a product (a surface salt film may form) or in-diffusion of a reactant (acceptor). Macrosmoothing also could occur under ohmic control for a sufficiently resistive electrolyte [12]. (2) Microsmoothing can also occur and is interpreted as a result of mass transport control, but at a smaller scale where diffusion is essentially isotropic. The salt film mechanism has been reported for polishing Ta in methanol-sulfuric acid [14].

Both EP and BCP chemistries use HF to convert the insoluble niobium oxide surface film to a soluble species, nominally written as $NbF_5$, though reality may be more complex. Describing either process as removing 100 μm of metal from the nominally one square meter interior surface of the cavity implies consumption of about 2 kg of 46% HF, if used at 100% efficiency. Certainly HF leaves the process in other ways than as $NbF_5$ from etching. Indeed non-etching HF loss is a significant process operations issue. Thus a more reasonable view of HF consumption may be a few kilos per cavity. In terms of 2008 world HF production of 679,000 tons, this amount is not large even for the sum of all envisioned SRF projects. Petroleum refinery use of HF as an alkylation catalyst for gasoline production and chemical industry use of HF as the fluorine source for fluorochemicals and fluoropolymers are far larger. However, all the SRF consumption leaves the Nb polishing process as toxic waste, none as product. Further, the industrial process use of HF occurs in well-contained continuous-operation vessels. The SRF use of HF occurs in individual multi-cell cavities, which must each be successively mounted and dismounted. A greater potential for error and for human exposure results. The cost of safe and environmentally responsible operation with HF certainly exceeds that required for other acids, though specific dollar values are hard to assess. A desirable alternative would be an HF-free process that delivers comparable SRF performance results. Efforts with molten organics salts are reported [15] but an actual process needs to be developed. Success with a methanol–magnesium perchlorate electrolyte was reported more than 30 years ago [16], but is excluded by its explosion potential. Since the construction of a major facility for EP of SRF cavities by the HF/sulfuric process is underway, it is especially desirable to develop an HF-free process that could be accommodated there with minimum adaptation. We therefore directed our attention to processes for which this might be possible.

In their extensive research on metals EP, the Landolt group at Lausanne investigated EP of tantalum [14, 17], a close chemical relative of niobium [18]. That work

employed 0.5–5 M sulfuric acid in methanol as an electrolyte in the −10 to 25 °C temperature range, using voltammetry, rotating disc electrode and EIS to observe behavior and investigate mechanisms. They found that the cell current depended linearly on the anode potential or was independent of potential (current plateau), indicating ohmic or mass-transfer control, respectively. Mass transfer control is believed to prevail under conditions desirable for EP [12]. The EIS and RDE results were interpreted to indicate rate control in the plateau region is by diffusion of Ta ions away from a compact salt film covering the surface. The voltage range for the current plateau was greatest at the lowest temperature and at 3 M acid concentration, with a current of about 160 mA $cm^{-2}$. Even a few tenths percent water in the electrolyte reduced the plateau current. Materials polished in the plateau current range were bright to the eye and atomic force microscopy (AFM) measurement showed an average roughness "on the order of 3 nm". Some particles were also seen, but not investigated. No information was provided about how the EP was terminated and if the specimens were then washed, raising the question of whether the particles might have been a remnant of the salt film.

In the present report, EP of Nb was performed in sulfuric acid–methanol electrolytes. The influences of sulfuric acid concentration, temperature, and EP duration on the system were investigated in a potentiostatically-controlled three electrode cell. EIS was performed in the three electrode set up. The resulting surfaces were examined by scanning electron microscopy (SEM), stylus profilometry (SP), atomic force microscopy (AFM) and x-ray photoelectron spectroscopy (XPS).

## 2 Experimental procedures

### 2.1 Preparation of samples

Polycrystalline Nb rods were cut from high-RRR-grade fine grain Nb sheet stock used at Thomas Jefferson National Laboratory to make SRF cavities. It has a purity of 99.9999% excluding Ta, according to the manufacture (Wah Chang, USA). The working electrodes were constructed by embedding the Nb rods into epoxy cylinders. The diameter of cylinders is about 10 mm. The exposed Nb area of the electrodes was approximately 0.4 $cm^2$. Prior to each electrochemical experiment, each Nb electrode was mechanically polished by 600 grit emery paper, rinsed in methanol, and dried in air. The counter electrode was a platinum foil and the reference electrode was a saturated mercurous sulfate electrode (MSE). All the potentials given below are with respect to the reference electrode. No correction for IR drops was applied to the measured polarization curves because the primary interest was the current plateau region.

The electrolytes were prepared from sulfuric acid (Certified ACS plus, 98%, Fisher Chemical) and methanol (HPLC grade, 99.9%, Fisher Chemical) and cooled while mixed. The $H_2SO_4$ concentrations in the methanol solutions were 0.5, 1, 2, and 3 M. Their maximum water content may be calculated from weight ratio and the sulfuric acid supplier's maximum water content as 0.21, 0.31, 0.49 and 0.66% by weight respectively. In the previous study of EP of Ta in methanol–sulfuric acid electrolytes, experimental determination of the water content for 3 M electrolyte prepared with similar supplier specifications gave a value of 0.2 wt% [14], while another EP work of Ti in methanol–sulfuric acid electrolytes found only a small effect on plateau current of water content in the 0.1–1 wt% range [19]. The electrolyte temperature in the present work was maintained at room temperature, 0, −10, or −30 °C. About 300 mL of fresh electrolyte was used for each experiment. The low temperature experiments were performed by placing the cell in a reservoir filled with ethanol whose temperature was controlled by an immersion cooler (EK45, Thermo Scientific Haake). A thermometer was inserted into the electrolyte to monitor the electrolyte temperature. The difference of temperature before and after EP was measured to be smaller than 2 °C.

### 2.2 Electrochemical measurements

Anodic polarization was controlled by a potentiostat (Model 263A, EG&G, Princeton Applied Research). The voltage was swept from 9–0 V at the rate of −10 mV $s^{-1}$. The negative scanning direction (high to low potential) was used to obtain a reproducible limiting current. The EP experiments were performed under potentiostatic conditions at 9 V. The volume of electrolyte for each EP process was about 300 mL, and no significant change in the volume was observed, even for duration up to 7 h. The plateau current during each EP process was kept constant for the duration; values are listed in Table 1. The weight loss of every electropolished Nb working electrode was recorded to estimate the average corrosion rate. In a further experiments metal removal of 100 μm, typical of SRF cavity polishing, and of 250 μm (to explore over-etching) were obtained. Nb taken into solution was about 0.2 mM/L for the 0.5 h experiments, 1.4 and 3.1 mM/L for the 100 and 250 μm removals, respectively.

EIS has been recently reviewed in depth [20] and specific application to elucidation of EP mechanisms was presented earlier [13]. The latter work describes an experimental approach in which data are collected at different applied potentials within the current limiting plateau. Plotting the data as real vs. imaginary impedance for an equivalent

**Table 1** Limiting current, estimated dissolution rate, corrosion rate, and thickness removal for EP at 9 V for 30 min under various condition combinations of $H_2SO_4$ concentration and temperature

| Sulfuric Acid Concentration (M) | Temperature ( °C) | Limiting current, $i$ (mA cm$^{-2}$) | Dissolution rate, $r'$ (μm min$^{-1}$) | Average corrosion rate, $r$ (μm min$^{-1}$) | Thickness removal (μm) |
|---|---|---|---|---|---|
| 0.5 | RT | 846 ± 22 | 11.4 | 10.3 | 310 |
| | 0 | 468 ± 28 | 6.3 | 6.2 | 186 |
| | −10 | 397 ± 16 | 5.4 | 5.4 | 160 |
| | −30 | 288 ± 15 | 3.9 | 4.1 | 123 |
| 1 | RT | 1013 ± 11 | 13.7 | 12.5 | 376 |
| | 0 | 457 ± 42 | 6.1 | 6.4 | 193 |
| | −10 | 428 ± 50 | 5.8 | 5.8 | 174 |
| | −30 | 271 ± 32 | 3.7 | 2.7 | 80 |
| 2 | RT | 596 ± 96 | 8.0 | 7.4 | 222 |
| | 0 | 166 ± 22 | 2.2 | 2.4 | 73 |
| | −10 | 150 ± 28 | 2.0 | 1.6 | 48 |
| | −30 | 63 ± 19 | 0.9 | 0.4 | 12 |
| 3 | RT | 181 ± 22 | 2.4 | 2.1 | 63 |
| | 0 | 38 ± 25 | 0.5 | 0.5 | 15 |
| | −10 | 66 ± 17 | 0.9 | 0.8 | 24 |
| | −30 | 34 ± 13 | 0.5 | 0.6 | 18 |

The dissolution rate is calculated from limiting current assuming 5 $e^-$ transfer reaction; the average corrosion rate and thickness removal are calculated from weight loss measurements

circuit (Nyquist plot, Fig. 7), provides access to values for the key parameters, from which the mechanism can be deduced. EIS measurements were performed in the current plateau region at constant potential using a frequency response analyzer (Solartron 1260) connected to a potentiostat (EG&G Princeton Applied Research Model 263A) and controlled by a computer interface. The reference was a MSE electrode. The Nb samples were conditioned at potential for 200 s before commencing EIS data collection. A 40 mV ac amplitude was used and a frequency range of 200–0.2 Hz. Each scan consisted of 10 s integration at each point and after a time delay of 1 s. Integration errors were observed at low frequencies resulting from an insufficient signal to noise ratio and from drift of the dc current density during dissolution; the present interpretations are based on the higher frequency data [21].

### 2.3 Surface characterization

Surface topography was examined by SEM, SP, and AFM. Preliminary indications of surface chemistry were obtained by XPS. The SEM work took advantage of fact that both topography and crystallographic orientation contribute to contrast in the back-scattered electron (BSE) signal, the latter being significantly weaker [22, 23]. The presence of orientation contrast alone in BSE images therefore indicates that smoothing has been achieved, though quantitative information about the degree of smoothness is not obtained. A Robinson backscatter detector (RBSD) on the LEO (Zeiss) 1550 was used to acquire the present data. Stylus profilometry (Alfa-Step 500, KLA-TENCOR) was performed to study the surface roughness. As a characterization of microsmoothing, the relationship between the root mean square of surface roughness ($R_{rms}$) and the measurement length scale was calculated. AFM measurements were performed with a Digital Instruments: Nanoscope IV AFM in tapping mode using silicon tips having a diameter of 10 nm. The samples were scanned in five different regions with scan sizes of $5 \times 5$ μm$^2$ and $50 \times 50$ μm$^2$. The XPS data were obtained using a PHI Ulvac "Quantera" instrument. All the work was performed at the Virginia Tech Nanoscale Characterization and Fabrication Laboratory, except for the AFM work at the William & Mary Applied Research Center Laboratory.

## 3 Results and discussion

### 3.1 Voltammetry

Figure 1 shows the anodic polarization data measured in sulfuric acid–methanol electrolytes with $H_2SO_4$ concentrations of 0.5, 1, 2, and 3 M at room temperature, 0, −10, and −30 °C. Well-pronounced limiting current plateaus are evident for multiple conditions, as reported previously for Ta and Ti in this electrolyte [14, 17, 19]. For 0.5 M electrolyte at room temperature, it is hard to observe a plateau in the current curve. On the contrary, the linear variation of current with potential indicates that ohmic resistance is current limiting. No polishing, but rather etching, is observed in this voltage range, as reported also for Ta and Ti [14, 17, 19]. The current drop appearing at the beginning

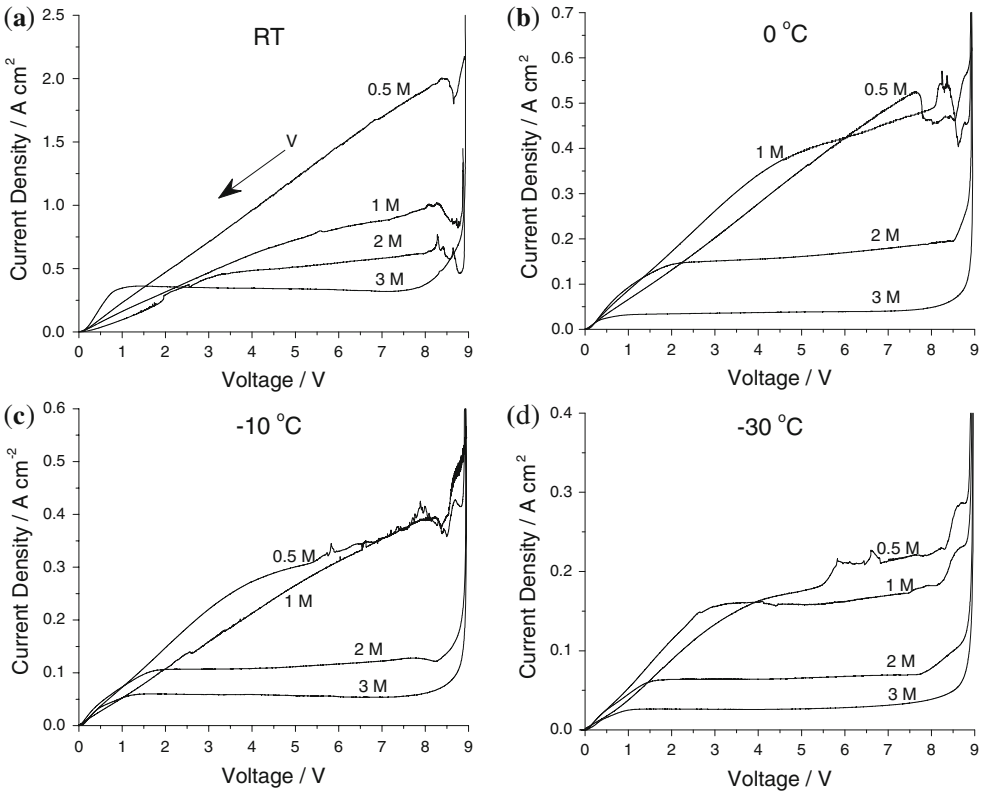


**Fig. 1** Nb I–V data measured in 0.5, 1, 2, and 3 M sulfuric acid–methanol electrolytes at **a** room temperature (RT), **b** 0 °C, **c** −10 °C, and **d** −30 °C. The scan rate was −10 mV s$^{-1}$; the *arrow* in **a** indicates the direction of voltage sweeping in all the measurements

of the voltage scan is consistent with the formation of an anodic film [14]. The 3 M electrolyte on the other hand displays a well-pronounced limiting current plateau extending from approximately 1–8 V. The surface after dissolution under conditions within the plateau appeared polished and bright to the unaided eyes.

The plateau value of the current decreases as the acid concentration increases, from 2 A cm$^{-2}$ (0.5 M, room temperature) to 0.3 A cm$^{-2}$ (3 M, room temperature). The decreasing plateau current is consistent with a decreasing solubility of metal ions, though some effect of greater water content cannot be excluded. A similar dependence on $H_2SO_4$ concentration was reported for EP of Ti, even when the water content was maintained below 0.02% for all [19]. Further, as the value of the plateau current decreases, the plateau voltage range expands from none (0.5 M, room temperature) to 7 V (3 M, room temperature).

The plateau current is also influenced by temperature (Fig. 1), decreasing most for the lowest acid concentration and almost not at all for the highest. With the decreasing temperature, we expect a decreased Nb ion solubility, an increased anodic film stability, and a decreased dissolution rate in the electrolyte. The plateau also expands with decreasing temperature; at −30 °C, all electrolytes display well-pronounced current plateaus.

Table 1 shows the limiting currents measured during EP of Nb as a function of temperature and acid concentration with an applied potential of 9 V for 30 min. The current value decreases as the acid concentration increases and the temperature decreases. There appears to be a transition of the plateau current from a larger value measured in lower acid concentrations of 0.5 and 1 M to a smaller value measured in higher acid concentrations of 2 and 3 M. These differences were also reflected in the final surface finishing.

The average current can be used to predict the dissolution rate of Nb by assuming the current is solely due to Nb dissolution. This dissolution rate ($r'$, μm min$^{-1}$) can be defined as:

$$r' = 6.22\frac{i \times M}{n \times \rho}, \tag{1}$$

where $M$ is the atomic weight of Nb (93 g mol$^{-1}$), $n$ is the oxidation state of Nb ions (assumed to be five), $t$ is the EP duration (min), $\rho$ is the density of Nb (8.57 g cm$^{-3}$), and $i$ is the average current density (A cm$^{-2}$).

Table 1 also shows the average corrosion rate and the thickness removal calculated from weight loss measurements for EP at 9 V for 30 min. The average corrosion rate ($r$, μm min$^{-1}$) is calculated by the equation:

$$r = \frac{\Delta m}{A \times \rho \times t}, \tag{2}$$

where $\Delta m$ is the weight loss (g), $A$ is the Nb electrode area (cm$^2$), $\rho$ is the density of Nb (8.57 g cm$^{-3}$), and $t$ is the EP

duration (min). The thickness removal is calculated by assuming a uniform Nb removal during EP (9 V, 30 min). Compared to HF-based methods, methanol-based EP resulted in a corrosion rate at least comparable to HF-based EP (0.5 μm $min^{-1}$). Furthermore, the corrosion rates are approximately equivalent to the estimated dissolution rates. This supports the notion that the recorded EP current is mainly composed of a 5 $e^-$ transfer Nb dissolution reaction.

### 3.2 Surface characterization

Preliminary XPS examination of surface chemistry after EP revealed no sulfur, only Nb, O and some adventitious carbon. Similar examination of materials processed by HF/sulfuric EP revealed no fluorine, but also only Nb, O and adventitious carbon. In contrast, materials processed by BCP showed fluorine concentrations in the range of a few to several percent of the oxygen.

Figure 2 shows SEM images of Nb surfaces electropolished in the 0.5 M electrolyte at 9 V for 30 min at room temperature and −30 °C. The corresponding thickness removals are shown in Table 1. Topographical contrast dominates for EP at room temperature while for EP at −30 °C the topographical features are sufficiently small that only orientation contrast is observed, indicating microsmoothing. Table 2 summarizes the surface finishing for various EP conditions. One can draw a conclusion that a higher $H_2SO_4$ concentration (e.g. 2 and 3 M) and a lower temperature (e.g. −30 °C) would be the favored condition for a microsmoothing.

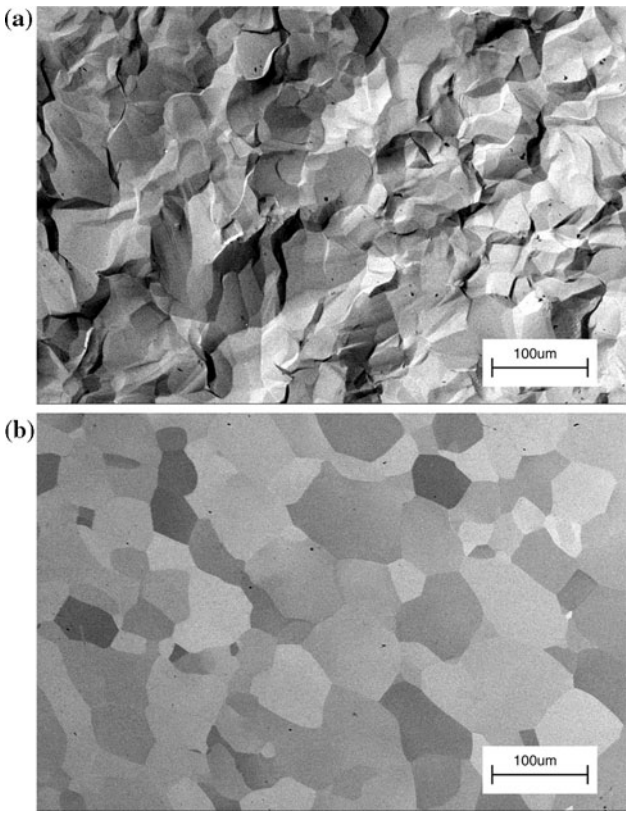


**Fig. 2** SEM images by using RBSD of Nb surfaces electropolished in the 0.5 M electrolyte at 9 V for 30 min at **a** room temperature and **b** −30 °C

**Table 2** Surface finishing observed for various EP conditions by SEM

| Sulfuric acid concentration (M) | Temperature (°C) | Topographic contrast | Orientation contrast |
|---|---|---|---|
| 0.5 | RT | X | |
| | 0 | X | |
| | −10 | X | |
| | −30 | | X |
| 1 | RT | X | |
| | 0 | | X |
| | −10 | | X |
| | −30 | | X |
| 2 | RT | | X |
| | 0 | | X |
| | −10 | | X |
| | −30 | | X |
| 3 | RT | | X |
| | 0 | | X |
| | −10 | | X |
| | −30 | | X |

**Table 3** $R_a$ determined by SP on Nb working electrodes electropolished at 9 V for 30 min under various EP condition combinations of $H_2SO_4$ concentration and temperature

| | 0.5 M | 1 M | 2 M | 3 M |
|---|---|---|---|---|
| RT | 2772 ± 566 | 2832 ± 1182 | **249 ± 63** | **703 ± 46** |
| 0 °C | 1517 ± 769 | **240 ± 78** | **134 ± 27** | **478 ± 36** |
| −10 °C | **548 ± 182** | **229 ± 92** | **204 ± 115** | **102 ± 18** |
| −30 °C | **298 ± 38** | **278 ± 118** | **132 ± 34** | **140 ± 27** |

Table 3 presents the average roughness ($R_a$) and standard deviation measured by SP profilometry for Nb electropolished at 9 V for 30 min under the same conditions as in Table 1. The scan length was 1 mm and the lateral resolution was 1 μm. The 1 M EP at room temperature, the 0.5 M EP at room temperature, and the 0.5 M EP at 0 °C resulted in a roughness on the scale of a few microns, smaller than the grain size. This finding indicates that no process was operating to bring about smoothening on this dimensional scale (no microsmoothing). Significant improvement is found under the conditions bold in Table 3. The $R_a$ values of these surfaces are of order of a few

100 nm and decreased with decreasing temperature. For these surfaces, only orientation contrast is observed in the SEM images. The I–V data for these conditions show well-pronounced current plateaus. The $R_a$ value over the 1 mm length scale indicates the degree of macrosmoothing.

For a more detailed understanding of the surface finishing at the microscopic scale, the relationship between $R_{rms}$ and measurement length scale was investigated by the model for variable length scale analysis developed by Chauvy et al. [24]. The $R_{rms}$ is defined as:

$$R_{rms} = \frac{1}{n_\varepsilon}\sum_{i=1}^{n_\varepsilon}\sqrt{\frac{1}{p_\varepsilon}\sum_{j=1}^{p_\varepsilon} h_j^2}, \tag{3}$$

where $n_\varepsilon$ is the number of intervals of a length of $\varepsilon$, $p_\varepsilon$ is the number of points in the length $\varepsilon$, $h_j$ is the height of the $j$-th point within the $i$-th interval ($1 \leq i \leq n_\varepsilon$). The value of $\varepsilon$ progresses from several microns to 1 mm.

Figure 3 shows the investigation on surface profile and $R_{rms}$ of surfaces electropolished in the 0.5 M sulfuric acid–methanol electrolyte at 9 V for 30 min. Figure 3a shows decreasing grain boundary height with decreasing temperature. The $R_{rms}$ shown in Fig. 3b also decreases along the whole length scale as the temperature decreases. On the microscopic scale (Fig. 3c)—the scale smaller than 200 μm—the $R_{rms}$ of the surface polished at −30 °C is only about 20 nm and remains constant. Since the 200 μm scale already covers several grains (the average size of grain is 50 μm), the constant $R_{rms}$ demonstrates that the polishing was completely uniform across this scale.

Figure 4 shows the results of microsmoothing in various acid concentrations. At room temperature (Fig. 4a), the $H_2SO_4$ concentration strongly influences the $R_{rms}$. The surface quality improves dramatically with increasing acid concentration. At −30 °C (Fig. 4c), the $R_{rms}$ corresponding to each acid concentration overlaps each other and is concentration-independent. The influence of $H_2SO_4$ concentration decreases with decreasing temperature. The temperature appears to be the more critical parameter for microsmoothing. However, the $R_{rms}$ values of surfaces polished in 2 and 3 M at −30 °C are not always smaller than those in 0.5 and 1 M. This may be the consequence of different total removal values for these conditions, resulting in less than total removal of mechanical damage. If this is true, then longer EP in the higher acid concentration (causing a sufficient thickness removal) is expected to result in a better surface finishing.

Table 4 presents the AFM results from materials polished at each $H_2SO_4$ concentration at −30 °C. These materials were chosen because the lowest temperature was expected to provide the best smoothening. Interestingly, $H_2SO_4$ concentration appears to make little difference. Data collected with scan lengths significantly smaller than

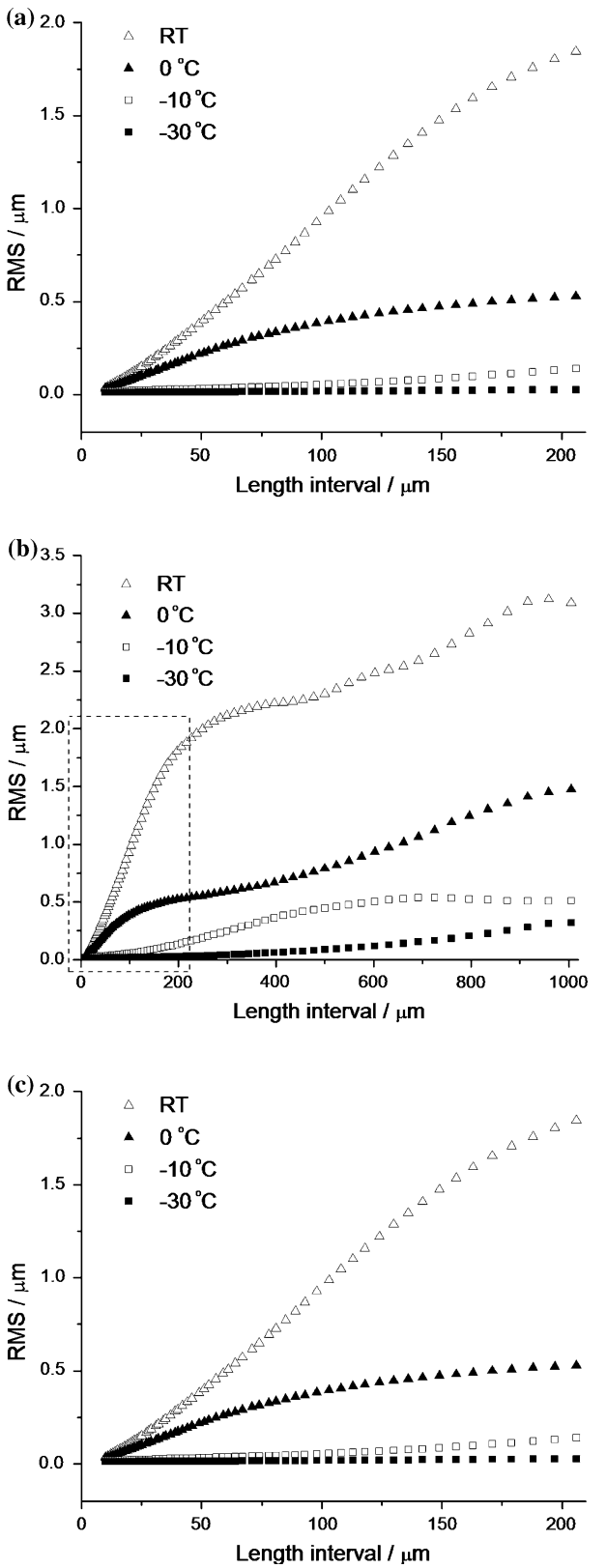


**Fig. 3** **a** Surface profile, **b** $R_{rms}$ as a function of length interval (1 mm), and **c** $R_{rms}$ as a function of length interval (0.2 mm, the *dash-lined region* in **b**) of Nb surfaces electropolished in the 0.5 M electrolyte at 9 V for 30 min

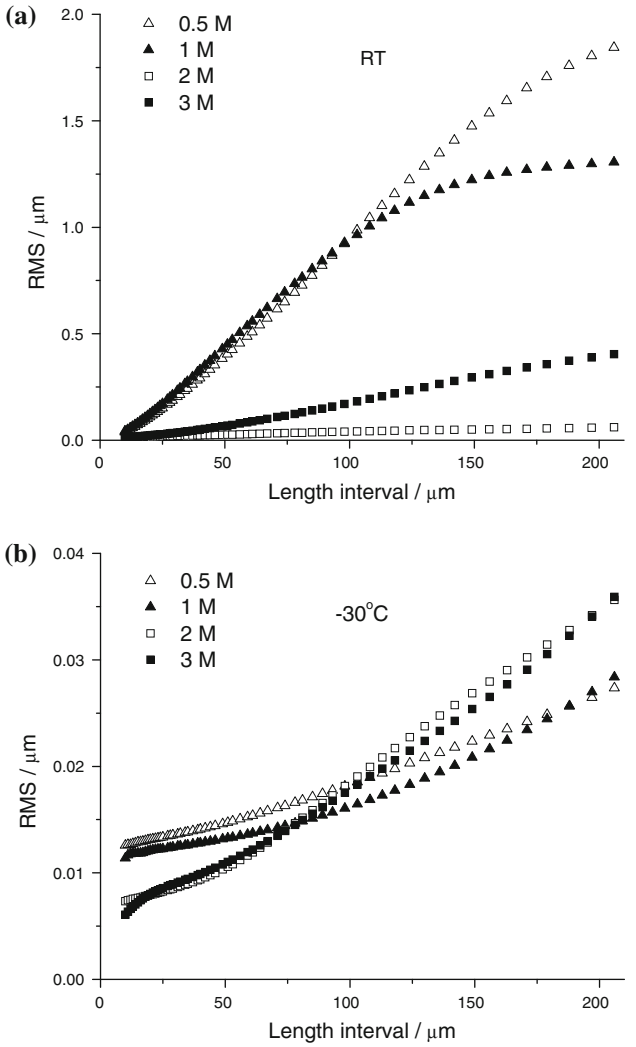


**Fig. 4** $R_{rms}$ as a function of length interval (0.2 mm) of Nb surfaces electropolished at 9 V for 30 min at **a** room temperature and **b** −30 °C

**Table 4** $R_a$ determined as an average of three AFM scans on Nb working electrodes electropolished in sulfuric acid–methanol electrolytes at 9 V for 30 min at −30 °C

| Sulfuric acid concentration (M) | $R_a$ (nm) 5 μm scans | $R_a$ (nm) 50 μm scans |
|---|---|---|
| 0.5 | 8.3 | 23.8 |
| 1 | 22.0 | 26.3 |
| 2 | 7.6 | 17.7 |
| 3 | 12.9 | 25.0 |
| HF/sulfuric | 2.1 | 35.9 |

the grain size tend to see less roughness than the longer scans, indicating that crystallographic etching is suppressed as would be expected for a surface salt film. The roughness at longer scale includes grain to grain effects, but still is similar to that obtained by HF sulfuric EP (47 nm for 20 μm scan [25]). The differences among all the samples are relatively small and probably are best not considered to be meaningful without much more extensive data. What seems to matter here is the presence or absence of polishing conditions. Large particles were seen here, as in the reported Ta work. Analysis by energy dispersive X-ray spectroscopy (EDS) in the SEM (data not shown) disclosed only niobium and oxygen.

### 3.3 Deep EP—long time potential hold

SRF cavity processing typically removes 100 μm of material, making this an important benchmark. The effect of over-etching under constant conditions is also of interest, here 250 μm. Loss of HF during laboratory experiments is a problem for over-etching experiments with HF sulfuric EP; such results appear not to have been reported. Here, EP was performed at 9 V for 3 or 7 h in the 3 M electrolyte at −30 °C. The resulting thickness removals were 113 and 252 μm (Table 5). Both showed the identical current and corrosion rate to the EP of 30 min, providing evidence of stable mass transport and a linear relationship between thickness removal and EP duration. SEM images (Fig. 5) captured on surfaces polished for various durations show that 100 μm removal indeed eliminates damage seen earlier. Macroscopic surface roughness measurements (Table 5) show this improvement by the smaller $R_a$ for longer EP. As the microscopic roughness characterization, Fig. 6 shows further suppression of grain boundary etching (Fig. 6a) and a decreasing $R_{rms}$ along the whole length scale for 3 h EP (Fig. 6b, c). Over-etching (7 h EP) appears to increase roughness, but more investigation than the single sample here is needed.

### 3.4 Impedance spectroscopy

The surface characterization indicates that EP performed in high $H_2SO_4$ concentration electrolytes and at low temperatures resulted in the microsmoothing, so the EIS data were obtained to indicate the mechanism. Figure 7a and b presents EIS data showing the influence of applied potential on the impedance diagram measured in the 2 and 3 M electrolytes at −30 °C. The applied potential was varied between from 3 to 8 V. Figure 7c interprets the equivalent circuit and corresponding Nyquist plot high frequency part of the impedance diagram. ZPlot software was used to calculate the solution resistance ($R_s$, the starting point of the semi-circle), the polarization resistance ($R_p$, diameter of the semi-circle), and double layer capacitance ($C_{dl}$, determined from the frequency $\omega$ at the top of the semi-circle and $R_p$ by $C_{dl} = 1/(\omega R_p)$). All calculated data are presented in Table 6. It is evident that $R_s$, representing the electrolyte

**Table 5** Parameters for electropolishing in the 3 M sulfuric acid–methanol electrolyte at 9 V for 30 min, 3, and 7 h at −30 °C

| Duration (h) | Limiting current (A $cm^{-2}$) | Corrosion rate (μm $min^{-1}$) | Thickness removal (μm) | Roughness ($R_a$, nm) |
|---|---|---|---|---|
| 0.5 | 0.034 ± 0.0128 | 0.63 | 19 | 140 ± 27 |
| 3 | 0.030 ± 0.0051 | 0.64 | 113 | 113 ± 11 |
| 7 | 0.031 ± 0.0041 | 0.60 | 252 | 120 ± 3 |

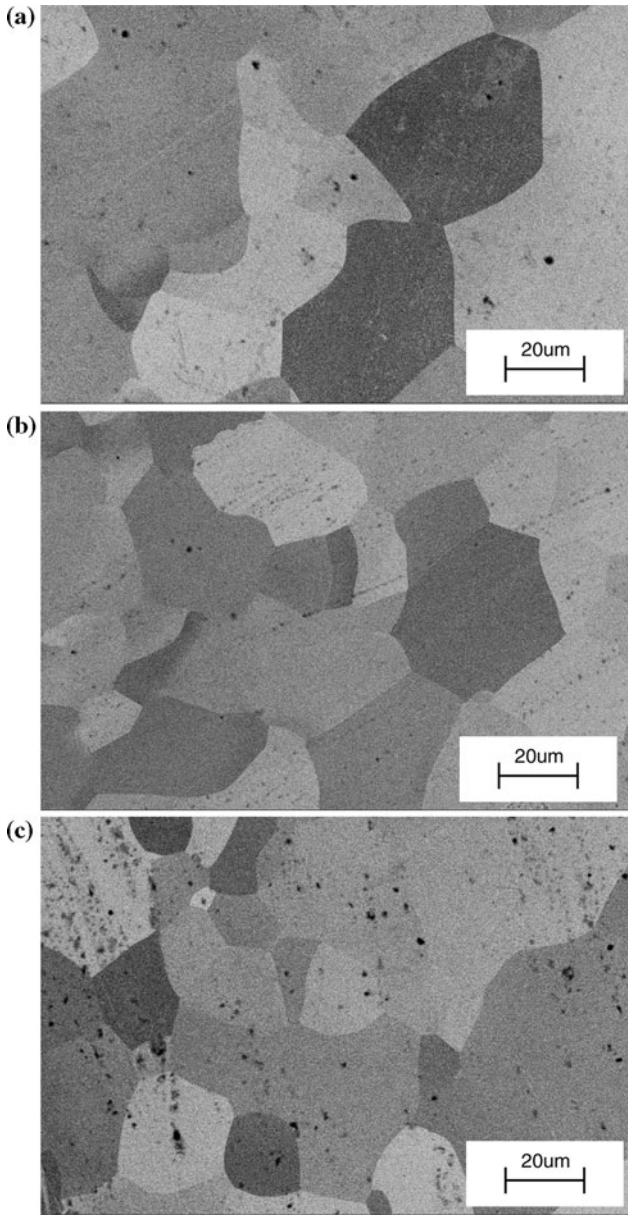


**Fig. 5** SEM images by using RBSD of Nb surfaces electropolished in the 3 M electrolyte at 9 V for **a** 30 min, **b** 3 h, and **c** 7 h at −30 °C

resistance between the reference electrode and the metal surface, remains constant; $R_p$ increases and $C_{dl}$ falls with increasing applied potential. Such behaviors are consistent only with the presence of a compact (salt) film on the anode surface [13]. Similar EIS data have been reported for Ta

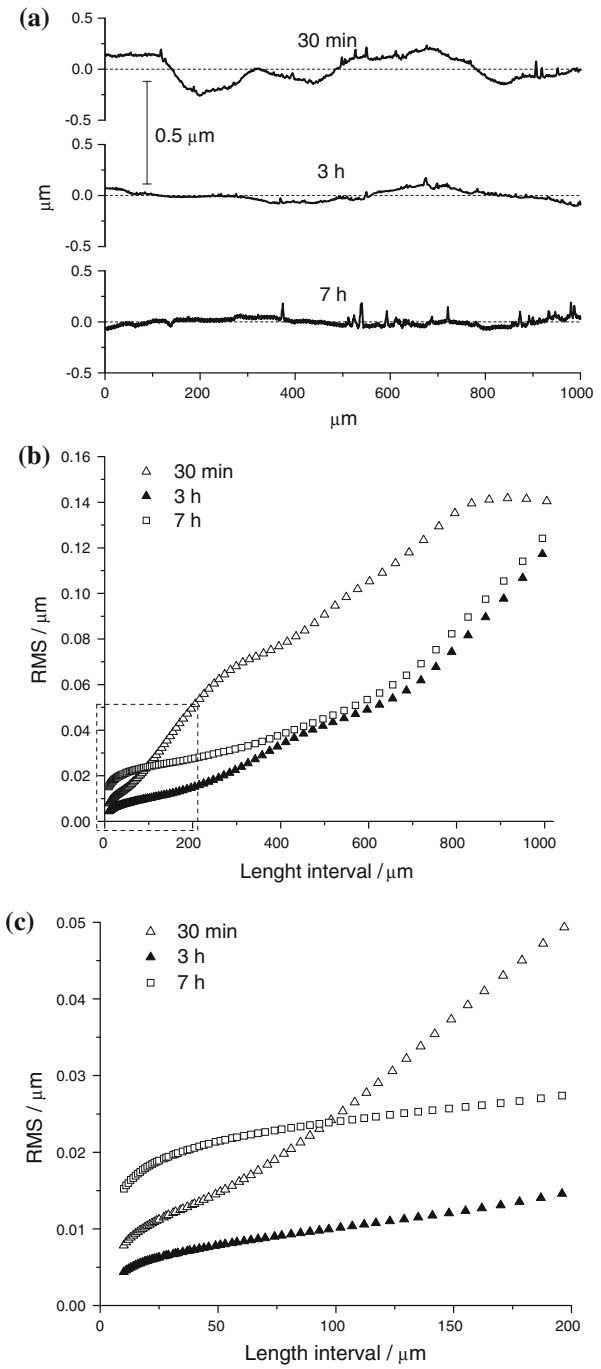


**Fig. 6** **a** Surface profile, **b** $R_{rms}$ as a function of length interval (1 mm), and **c** $R_{rms}$ as a function of length interval (0.2 mm, the *dash-lined region* in **b**) of Nb surfaces electropolished in the 3 M electrolyte at 9 V for 30 min, 3, and 7 h at −30 °C

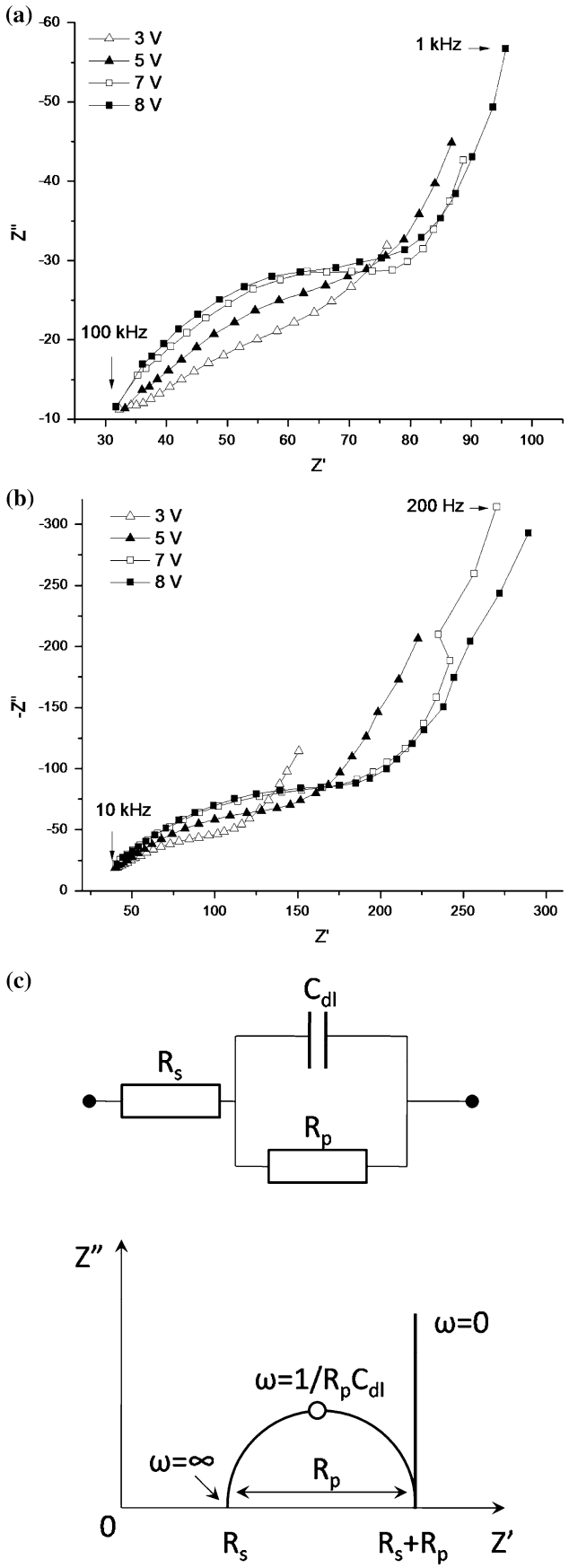


◀ **Fig. 7** Nyquist diagram showing the effect of applied potential on the impedance measured in the **a** 2 M and **b** 3 M electrolytes at −30 °C, **c** equivalent circuit (*upper*) and corresponding Nyquist plot for the interpretation of the high frequency part of the impedance diagram (*lower*)

**Table 6** Parameters estimated from the EIS measurements in the 3 and 2 M electrolytes at −30 °C

| Sulfuric acid concentration (M) | Potential (V) | $R_s$ (Ω cm$^2$) | $R_p$ (Ω cm$^2$) | $C_{dl}$ (μF) |
|---|---|---|---|---|
| 2 | 8 | 31.8 | 56.8 | 0.227 |
| | 7 | 31.8 | 55.3 | 0.246 |
| | 5 | 32.2 | 46.5 | 0.293 |
| | 3 | 32.3 | 29.7 | 0.438 |
| 3 | 8 | 40.9 | 163.0 | 0.164 |
| | 7 | 40.5 | 152.4 | 0.181 |
| | 5 | 40.3 | 118.5 | 0.285 |
| | 3 | 39.6 | 109.7 | 0.555 |

and Ti in this electrolyte [14, 19] and Nb in HF–$H_2SO_4$ electrolyte [11].

## 4 Conclusions

HF-Free EP of Nb was performed in sulfuric acid–methanol electrolytes with $H_2SO_4$ concentrations of 0.5, 1, 2, and 3 M. Anodic polarization and potential hold experiments were performed to evaluate the electrochemical process. A current plateau was found. The plateau current decreased in value and the plateau voltage range increased with increasing $H_2SO_4$ concentration and decreasing temperature. The metal removal rate under conditions that gave the best polishing was comparable to that obtained by HF–$H_2SO_4$ EP. Examination of these materials by several techniques showed that both macrosmoothing and microsmoothing were obtained. Temperature is determined to be a more critical parameter than $H_2SO_4$ concentration to achieve microsmoothing. With decreasing temperature, the surface quality improved substantially. At −30 °C, microsmoothing was achieved in all $H_2SO_4$ concentrations. For a desired material removal of 100 μm, the surface mechanical damage was completely removed and a nanometer-scale surface roughness was measured. The EIS findings point to a compact salt film being responsible for the presence of the current plateau. Equivalent findings for EP of chemically-similar tantalum with this electrolyte were interpreted as due to mass transfer limitation by diffusion of Nb ions away from the surface. We infer that a similar mechanism is at work here.

**Acknowledgments** This research work was supported by the US Department of Energy under grant DE-FG02-06ER41434 to Virginia Tech. We thank the SRF Institute at Jefferson Lab for providing the niobium rods, and niobium specimens treated by fluoride-based EP and by BCP. We thank the Nanoscale Characterization and Fabrication Laboratory at Virginia Tech for assistance with scanning electron microscopy, stylus profilometry and x-ray photoelectron spectroscopy. We thank Olga Trofimova of the College of William and Mary for assistance with atomic force microscopy.

## References

1. Padamsee H, Knobloch J, Hays T (2008) RF superconductivity for accelerators, 2nd edn. Wiley, New York
2. Padamsee H (2009) RF superconductivity: science, technology and applications. Wiley, Weinheim
3. Knobloch J, Geng RL, Liepe M, Padamsee H (1999) In: Proc. 9th workshop on RF superconductivity, Ithaca
4. Saito K (2003) SRF2003 http://srf2003.desy.de/fap/paper/ThP15.pdf
5. Shemelin V, Padamsee H (2008) TTC Report 2008-07 TESLA
6. Tian H, Reece C, Kelley M, Wang S, Plucinski L, Smith K (2006) Appl Surf Sci 253:1236
7. Diepers H, Schmidt O, Martens H, Sun FS (1971) Phys Lett 37A:139
8. Saito K, Kojima Y, Furuya T, Mitsunobu S, Noguchi S, Hosoyama K, Nakazato T, Tajima T, Asano K, Inoue K, Iino Y, Nomura H, Takeuchi K, (1989) In: Proc. 4th workshop on RF superconductivity 2 KEK, Tsukuba
9. Geng, Crawford AC, Padamsee H, Seaman A (2005) In: Proc. 9th workshop on RF superconductivity, Ithaca
10. Padamsee H, Crawford AC, Favale A, Cole M, Rathke J, Pekeler M, Ashmanskas W (2007) In: Proc. PAC 07, Albuquerque
11. Tian H, Kelley M, Reece C, Corcoran S (2008) J Electrochem Soc 155:D563
12. Landolt D (1987) Electrochim Acta 32:1
13. Matlosz M (1995) Electrochim Acta 40:393
14. Piotrowski O, Madore C, Landolt D (1999) Electrochim Acta 44:3389
15. Palmieri V, Mondin G, Rampazzo V, Rizzetto D, Rupp V, Stivanello S, Deambrosis S, Rossi AA (2009) In: Proc. SRF 2009, Berlin, THOAAU03
16. Schober T, Sorajic V (1973) Metallography 6:183
17. Piotrowski O, Madore C, Landolt D (1998) Plat Surf Finish 85:115
18. Lupton D, Aldinger F, Schulse K (1981) In: Niobium: Proc Intl Symp 1981, San Francisco
19. Piotrowski O, Madore C, Landolt D (1998) J Electrochem Soc 145:2362
20. Orazem ME, Tribollet B (2008) Electrochemical impedance spectroscopy. Wiley, Hoboken
21. Grimm R, Landolt D (1994) Corros Sci 36:1847
22. Goldstein J, Newbury D, Joy D, Lyman C, Echlin P, Lifshin E, Sawyer L, Michael J (2007) Scanning electron microscopy and x-ray microanalysis, 3rd edn. Springer, New York
23. Verhoeven JD (1986) ASM handbook, vol 10, p 490. ASM International, Materials Park, OH, USA
24. Chauvy PF, Madore C, Landolt D (1998) Surf Coat Technol 110:48
25. Tian H, Ribeill G, Reece C, Kelley M (2011) Appl Surf Sci 257:4781